

Thermodynamics of the hydrophobic effect. I. Coupling of aggregation and pK_a shifts in solutions of aliphatic amines

Daumantas Matulis*, Victor A. Bloomfield

*Department of Biochemistry, Molecular Biology, and Biophysics, University of Minnesota, 1479 Gortner Ave., Saint Paul,
MN 55108, USA*

Received 29 May 2001; received in revised form 31 July 2001; accepted 31 July 2001

Abstract

Long aliphatic hydrocarbon chains aggregate in aqueous solution due to the hydrophobic effect, forming structures such as micelles and membranes, while amino groups titrate at basic pH. These two biologically important behaviors are linked in alkylamines, in which the pK_a of the amino group is shifted downward by aggregation. In this paper we study the thermodynamics of these coupled processes, following aggregation by observing alkylamine pH titration behavior. The magnitude of the shift depended on the aliphatic chain length and on the concentration of alkylamine: longer chains and higher concentrations lowered the pK_a to a greater extent. Gibbs free energies of protonation and aggregation were calculated from the pK_a shifts. Enthalpies, entropies, and heat capacities were estimated by van't Hoff analysis from the pK_a shift dependencies on temperature. However, the results were less precise than the calorimetrically measured values, as described in the following article. A model to calculate titration curves, pK_a shifts, and aggregation of uncharged alkylamines as a function of aliphatic chain length, concentration, and temperature is presented. © 2001 Elsevier Science B.V. All rights reserved.

Keywords: Dodecylammonium chloride; Alkylammonium pK_a shift; Thermodynamics of molecular interactions; Van't Hoff enthalpy; Calorimetric enthalpy; Isothermal titration calorimetry

* Corresponding author. Tel.: +1-612-624-7468; fax: +1-612-625-5780.
E-mail address: dmatulis@biosci.umn.edu (D. Matulis).

1. Introduction

Determination and interpretation of ionizable group pK_a values is an important subject in biological chemistry [1]. Protein ionizable group pK_a values are widely used for the calculation of electrostatic interactions in proteins [1–3], and shifts in pK_a values of ionizable amino acid side chains are an important source of information about neighboring charges and dipoles, dielectrical permittivity and hydration of the environment of the amino acid [4].

One of the less recognized reasons for pK_a shifts is association and aggregation of molecules in solution. This occurs for long chain alkylamines. Protonation constants of short chain alkylamines with 1–6 carbon atoms were determined over a century ago. Both the protonated and deprotonated amine forms were fully soluble in water. However, it was noticed that longer chain alkylamines aggregate upon deprotonation. Deprotonated forms of alkylamines such as dodecylamine were practically insoluble in water. These difficulties prevented determination of the pK_a values of long chain alkylamines in water. Hoerr et al. [5] determined long chain aliphatic amine (9–18 carbon atoms) pK_a values by measuring equivalent conductance in various ethanol–water mixtures and extrapolating to zero ethanol concentration. This method prevented aggregation of deprotonated amine.

However, recent compilations of pK_a values of organic compounds do not elaborate on the method of pK_a determination [6–8]. These, and other similar sources simply list all pK_a values. Therefore, it appears from recent tabulations that, for example, the pK_a values of methylamine and tetradecylamine in aqueous solution are equal (10.63 for methylamine and 10.62 for tetradecylamine [7]). This would be true in the infinitely dilute solutions. However, observable pK_a values in aqueous solution are very different.

In this study we investigate the linked protonation and aggregation equilibria of long chain (10–14 carbon atoms) aliphatic amines (1-amino-*n*-alkanes) in aqueous solution by potentiometric titration. Such an approach enables determina-

tion of both the aggregation and ionization thermodynamics. The aggregation reaction is fully reversible as demonstrated by back-titration, thus the system is in thermodynamic equilibrium. Furthermore, the pK_a of the soluble amine is the same for all chain lengths, but the observed pK_a is precisely predictable from alkylamine solubility data. Conversely, the observed pK_a can be used to determine the Gibbs free energy of aggregation, a quantity difficult to determine directly by solubility measurements because of linked ionization equilibrium.

Other thermodynamic functions of aggregation, including enthalpy, entropy, and heat capacity, were estimated from the temperature dependence of the pK_a shift by using van't Hoff analysis. The main conclusions were consistent with the aliphatic alkane aggregation thermodynamics as determined by van't Hoff analysis of alkane solubilities [9]. It is not possible to determine alkane aggregation thermodynamics in aqueous solution by titration calorimetry at a constant temperature and pressure. However, it was possible to carry out such experiments with alkylamines using the linked protonation equilibrium. Thermodynamic parameters of aggregation determined by titration calorimetry [10] were found to be largely inconsistent with the van't Hoff analysis, because the precision of the pK_a shift and solubility data is insufficient to yield meaningful results. These results lead to reconsideration of the thermodynamics of hydrophobic interactions between long aliphatic chains [11].

2. Methods

2.1. Chemicals

Most alkylamines including propylamine hydrochloride, propylamine, octylamine, nonylamine, decylamine, undecylamine, dodecylamine, tridecylamine, and tetradecylamine were purchased from Aldrich Chemical Co. (Milwaukee, WI). Octylamine hydrochloride and dodecylamine hydrochloride were purchased from Acros Organics (currently obtainable through Fisher Scientific).

All alkylamines were at least 98% pure, and were used without further purification. All other chemicals were of the reagent grade.

2.2. Potentiometric titration of alkylamines

Alkylamine solutions of various concentrations were prepared by adding HCl to the exactly same amount of non-ionic amine to fully protonate amine to the alkylammonium cation. To all solutions 10.0 mM NaCl was added to maintain non-zero ionic strength. Such alkylammonium solutions were titrated with 10 times more concentrated NaOH solutions containing 10.0 mM NaCl, and then backwards with HCl solution of the same concentration (in 10 mM NaCl) to confirm reversibility. Alkylamine concentrations used were 1, 2, 5 and 10 mM, and they were titrated with 10, 20, 50 and 100 mM NaOH and HCl solutions, respectively. pH was measured potentiometrically using a Beckman Research pH meter with the error less than 0.01 pH units and calibration uncertainty of approximately 0.1 pH units. Titration reactions were carried out in a temperature-controlled water bath at 24.3, 34.3, 43.1 and 53.4°C. The deviation in temperature was approximately $\pm 0.3^\circ\text{C}$ and did not exceed $\pm 0.8^\circ\text{C}$ during the titration. Experiments were repeated several times to estimate an error of measurement. The pH meter was calibrated with 50 mM sodium carbonate buffer (25 mM Na_2CO_3 /25 mM NaHCO_3). However, there is a slight discrepancy about the pH of such solution in several literature sources. Butler and Cogley [12] list the pH values of 10.012 and 10.329 of the same buffer at 25°C and zero ionic strength. We used the following pH values to calibrate the pH meter at our experimental temperatures and small ionic strengths: 24.3°C — 10.23, 34.3°C — 10.16, 43.1°C — 10.10, 53.4°C — 10.05. Furthermore, the pH meter was checked with 0.1 M fresh NaOH. The deviation was always less than ± 0.1 pH units from the following expected pH values [13]: 24.3°C — 12.91, 34.3°C — 12.59, 43.1°C — 12.31, 53.4°C — 12.06. Alkylamines with 11–14 carbon atoms visibly aggregated upon deprotonation by sodium hydroxide, but fully redissolved upon protonation with hydrochloric acid during back-titration. The titra-

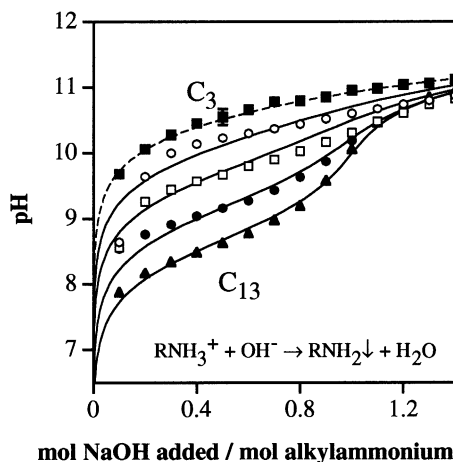


Fig. 1. Potentiometric titration curves of alkylammonium chlorides (2 mM) with sodium hydroxide (20 mM). Datapoints are the experimentally observed results: ■, propylammonium (C_3); ○, decylammonium (C_{10}); □, undecylammonium (C_{11}); ●, dodecylammonium (C_{12}); and ▲, tridecylammonium (C_{13}). Lines are calculated according to the model (see text). Dotted line — propylamine titration, practically unperturbed by aggregation. Solid lines — titration of longer chain alkylamines with the midpoints (protonation pK_a values) shifted downwards due to the aggregation.

tion curves shown in Figs. 1, 2 and 7 were obtained by titration with NaOH. Nearly identical curves were obtained by back-titration with HCl indicating that the aggregation reaction was fully reversible and the observed pK_a values represented true thermodynamic equilibrium.

3. Results

3.1. Observed pK_a values of long-chain aliphatic amines by potentiometric titration

Positively charged *n*-alkylammonium chlorides with various alkyl chain lengths were titrated with sodium hydroxide. There was no aggregation of short alkylamines, such as propylamine. However, long chain alkylamines, such as tetradecylamine, visibly aggregated in aqueous solution upon deprotonation. The symbols in Fig. 1 show potentiometric titration curves of deprotonation and aggregation of long chain alkylamines. The lines are

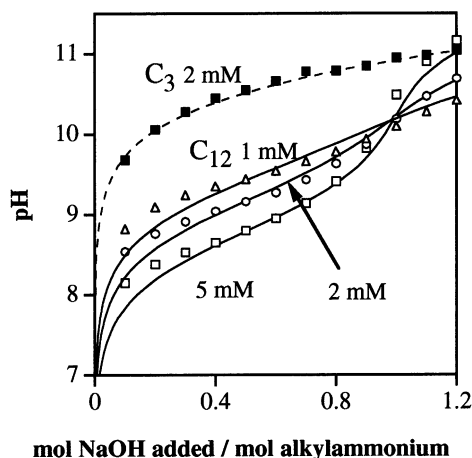


Fig. 2. Potentiometric titration curves of propylammonium (■, dotted line, C_3) and dodecylammonium (solid lines, C_{12}) chlorides with sodium hydroxide at various concentrations: Δ , 1 mM; \circ , 2 mM; \square , 5 mM. Propylamine titration curve was practically independent of concentration. Datapoints are the experimentally observed results, and the lines are calculated according to the model. Propylamine titration was unperturbed by aggregation. Solid lines — titration of dodecylamine with the midpoints (protonation pK_a values) shifted downwards due to aggregation.

calculated according to the model that will be discussed later. The midpoints of the titration curves, which are the observed pK_a values, pK_{obs} , were shifted towards lower pH values for longer chain alkylamines. The longer the aliphatic chain, the greater was the downward shift of the titration curve. Every additional methylene group shifted the pK_{obs} value downwards by approximately 0.6–0.8 pH units.

To make sure that such shift of the titration curves is not due to a kinetic effect of trapping the aggregated form of the amine, the reverse titration was performed. Back-titration of the aggregate with hydrochloric acid yielded practically identical titration curves and pK_{obs} values for each alkylamine. Therefore, both the protonation–deprotonation and the aggregation–dissolution reactions were fully reversible, showing that the experiments were carried out under thermodynamic equilibrium conditions. Repeatability of the titrations was also good, with an average standard error of approximately 0.1 pH unit.

The shift in the pK_{obs} was also dependent on the total added alkylamine concentration, being greater at higher concentrations of alkylamines. Fig. 2 shows dodecylamine (C_{12}) titration curves at various concentrations and the propylamine (C_3) control curve. The propylamine titration curve essentially did not vary with concentration, while the dodecylamine titration curve shifted more when higher concentrations were used. These observations correlated with aggregation: dodecylamine aggregated upon deprotonation and propylamine did not.

3.2. Ionization equilibria

Three reactions occur upon titrating protonated amines with sodium hydroxide: alkylammonium cation is deprotonated; hydroxide anion is protonated; and uncharged alkylamine aggregates to an extent that depends on alkyl chain length and concentration:



The alkylamine protonation constant is:

$$K_{acid} = \frac{[RNH_2][H^+]}{[RNH_3^+]} = 10^{-10.64} \\ = 2.29 \times 10^{-11} \text{ M} \quad (4)$$

This value comes from literature sources (Table 1), which conclude that in the absence of aggregation, the alkylamine protonation equilibrium constant is equal to $10^{-10.64}$, and the pK_{acid} is equal to 10.64 ± 0.1 . It is independent of alkylamine concentration and the alkyl chain length from 1 to 18 carbon atoms [5,14]. However, K_{acid} values for long chain alkylamines were estimated by measuring equivalent conductivities of alkylamines in the presence of various alcohol concentrations, and then extrapolated to zero alcohol concentration. By doing so, aggregation was prevented. Instead, in this article, we are interested

Table 1

The shift of long chain alkylamine protonation pK_a values as a function of alkyl chain length (m) and alkylamine concentration (C)

m^a	C^b (mM)	pK_{a-lit}^c	pK_{a-lit}^d	pK_{obs}^e	pK_{calc}^f
1	–	10.63	10.6532	–	10.64
2	–	10.70	10.6784	–	10.64
3	2	10.60	10.5685	10.65 ± 0.10	10.64
4	–	10.77	10.6385	–	10.64
5	–	10.63	10.631	–	10.64
6	–	10.56	10.639	–	10.64
7	–	10.67	–	–	10.63
8	–	10.65	–	–	10.60
9	–	10.64	10.64	–	10.50
10	2	10.64	10.64	10.23 ± 0.10	10.23
11	2	10.63	10.63	9.67 ± 0.12	9.76
12	2	10.63	10.63	9.13 ± 0.10	9.18
13	2	10.63	10.63	8.50 ± 0.15	8.56
14	2	10.62	10.62	7.56 ± 0.25	7.93
12	1	10.63	10.63	9.44 ± 0.10	9.46
12	2	10.63	10.63	9.16 ± 0.10	9.18
12	5	10.63	10.63	8.80 ± 0.15	8.79
12	10	10.63	10.63	8.73 ± 0.20	8.49

^aNumber of carbon atoms in alkylamine (e.g. $m = 12$, dodecylamine).^bTotal added concentration of alkylamine at the beginning of titration at which our experimental pK_a values were determined.^cAlkylamine protonation pK_a values as listed in a databook [7] without explanation how they were measured (pK_a values are concentration-independent).^dAlkylamine protonation pK_a values as determined in aqueous solution (1–6 carbon atoms) [14], or with various concentrations of ethanol (9–14 carbon atoms), preventing aggregation of long amines [5] (pK_a values are concentration-independent).^eOur experimental pK_a values in aqueous solution allowing aggregation (pK_a values are concentration-dependent).^fAlkylamine protonation pK_{calc} as calculated using Eq. (17).

in quantifying the effect of aggregation on protonation.

3.3. Alkylamine solubility and aggregation

The concentration of soluble amine can be written as:

$$[RNH_2] = fS = S \frac{[RNH_2 \downarrow]}{C} \quad (5)$$

where S is the limiting solubility of RNH_2 , f is the fraction of RNH_2 in precipitated form, and C is the total concentration of alkylamine in all forms:

$$C = [RNH_3^+] + [RNH_2] + [RNH_2 \downarrow] \quad (6)$$

Here $[RNH_2 \downarrow]$ is to be understood as the moles of precipitate per liter of solution, not the local concentration of precipitated alkylamine. Eq. (5), while approximate, is physically reasonable and numerically adequate over its range of application.

3.4. Gibbs free energy of aggregation

We now define aggregation ‘equilibrium constant’, A , as the reciprocal of the solubility:

$$A = \frac{1}{S} = \frac{[RNH_2 \downarrow]}{[RNH_2] \cdot C} \quad (7)$$

or in another form we express the precipitation equilibrium as a function of C and A :

$$\frac{[\text{RNH}_2 \downarrow]}{[\text{RNH}_2]} = AC$$

A is related to the Gibbs free energy of aggregation, the free energy of transferring 1 mol of dissolved RNH_2 (at infinite dilution, 1 M standard state) to the precipitated phase:

$$\Delta_A G = -RT \ln A = RT \ln S \quad (8)$$

It has been approximated for a long time [9] that the Gibbs free energy of aggregation of linear n -alkanes, 1-alcohols, and 1-amino alkanes depends linearly on the aliphatic chain length:

$$\Delta_A G(m) = -RT(m \ln \Delta \omega + \ln \omega_0) \quad (9)$$

so

$$A = \omega_0 \cdot \Delta \omega^m \quad (10)$$

Here m is the number of carbon atoms in the aliphatic chain, and the factors $\Delta \omega$ and ω_0 are empirically determined by linear regression of experimental solubility data [11,15–17]. The factor $\Delta \omega$, by which the aggregation equilibrium constant increases upon adding one methylene (CH_2) group to the alkyl chain has been determined to be approximately equal to 4.241 for all classes of linear aliphatic compounds. The coefficient ω_0 which reflects head group contributions, is equal to 1.32 for alkanes, 0.00309 for alcohols, and 0.000416 for alkylamines [11]. Values of A as calculated by Eq. (10) are listed in Table 2.

3.5. Calculation of alkylamine titration curves

We now use the alkylamine protonation and aggregation equilibria, along with other equilibria and conservation relations, to predict the titration

Table 2

Aggregation parameters, A , and the comparison between the two Gibbs free energies of aggregation ($\Delta_A G$ and $\Delta_{\text{agg}} G$) for alkylamines with m carbon atoms per molecule and alkylamine concentration C

m^a	C^b (mM)	A^c (M^{-1})	$\Delta_A G^d$ (kJ mol^{-1})	$1 + AC^e$	$\Delta_{\text{agg}} G^f$ (kJ mol^{-1})	$\Delta_{\text{calc}} G^g$ (kJ mol^{-1})
3	2	0.0317	8.56	1.00	−0.00016	60.7
4	—	0.134	4.97	1.00	−0.00067	60.7
5	—	0.57	1.39	1.00	−0.00283	60.7
6	—	2.42	−2.19	1.00	−0.0120	60.7
7	—	10.3	−5.77	1.02	−0.0503	60.7
8	—	43.5	−9.35	1.09	−0.207	60.5
9	—	184	−12.93	1.37	−0.779	60.0
10	2	782	−16.52	2.56	−2.33	58.4
11	2	3320	−20.10	7.64	−5.04	55.7
12	2	14 100	−23.68	29.2	−8.36	52.4
13	2	59 700	−27.26	120.4	−11.9	48.9
14	2	253 000	−30.84	507	−15.4	45.3
12	1	14 100	−23.68	15.1	−6.73	54.0
12	2	14 100	−23.68	29.2	−8.36	52.4
12	5	14 100	−23.68	71.5	−10.6	50.2
12	10	14 100	−23.68	142	−12.3	48.5

^a Number of carbon atoms in alkylamine (e.g. $m = 12$, dodecylamine).

^b Total added concentration of alkylamine [C , Eq. (6)].

^c Aggregation equilibrium parameter A as calculated using Eq. (10).

^d Gibbs free energy of aggregation calculated using Eq. (9).

^e Aggregation equilibrium parameter Agg .

^f Gibbs free energy of aggregation as calculated using Eq. (20).

^g Overall Gibbs free energy of deprotonation in the presence of aggregation [Eq. (19)].

curves shown in Figs. 1, 2 and 7, a test of our model.

The dissociation product of water is:

$$K_w = [H^+][OH^-] = 10^{-14} \text{ M}^2 \text{ at } 25^\circ\text{C} \quad (11)$$

Charge balance must be preserved at any stage of titration:

$$\begin{aligned} [H^+] + [Na_{\text{add}}^+] + [RNH_3^+] \\ = [OH^-] + [Cl^-] \end{aligned} \quad (12)$$

The added Na^+ concentration is equal to the added OH^- concentration because these ions are being added together:

$$[Na_{\text{add}}^+] = [OH_{\text{add}}^-] \quad (13)$$

The chloride concentration is equal to the initially added alkylammonium concentration and thus to the sum of all amine species at any stage of titration [Eq. (6)]:

$$C = [Cl^-] \quad (14)$$

The total Na^+ and Cl^- concentrations are higher in our experiments than indicated from Eq. (13) to Eq. (14), since there is a constant additional concentration of $NaCl$ of 10 mM in both the titrant and the titrating solutions to maintain approximately constant ionic strength during titration. These added concentrations cancel out of the equations.

We now have the seven equations [Eqs. (4), (6), (7), (11)–(14)] needed to calculate the concentrations of the seven species in the equilibria — $[RNH_3^+]$, $[RNH_2]$, $[RNH_2 \downarrow]$, $[Na^+]$, $[OH_{\text{add}}^-]$, $[OH^-]$, and $[H^+]$ — in terms of the parameters K_{acid} , K_w , A , and C , and thereby predict the titration curves. Algebraic manipulation yields a cubic equation, which can be rearranged to calculate $pH = -\log[H^+]$ as a function of added sodium hydroxide $[OH_{\text{add}}^-]$. To avoid solving the cubic equation we instead express $[OH_{\text{add}}^-]$ as a function of pH :

$$\begin{aligned} [OH_{\text{add}}^-] = & -[H^+]^3 - (AC + 1)K_{\text{acid}}[H^+]^2 \\ & + (K_w + (AC + 1)CK_{\text{acid}})[H^+] \\ & + (AC + 1)K_{\text{acid}}K_w \\ & ([H^+]^2 + (AC + 1)K_{\text{acid}}[H^+])^{-1} \end{aligned} \quad (15)$$

which yields the calculated lines in Figs. 1, 2 and 7. Within the standard error of the measurements, the experimental datapoints were generally well fitted by the calculated lines, without any further adjustment of the parameters. For the mathematical solution of similar ionic equilibria see Butler and Cogley [12].

3.6. Calculation of the alkylamine pK_a shifts

The observed pK_a values (the midpoints of the titration curves) can be calculated by adding the equations:

$$[RNH_3^+] = [RNH_2] + [RNH_2 \downarrow] = \frac{C}{2} \quad (16)$$

Solving the system of Eqs. (4), (6), (7), (11)–(14) and (16) for pH at the midpoints of the titration curves gives the simple result:

$$pH_{\text{midp}} = pK_{\text{calc}} = pK_{\text{acid}} - \log(AC + 1) \quad (17)$$

and the effective protonation equilibrium constant is:

$$K_{\text{calc}} = K_{\text{acid}}(AC + 1) \quad (18)$$

or

$$K_{\text{calc}} = K_{\text{acid}} Agg$$

where $Agg = AC + 1$. The Agg parameter describes the equilibrium of an aggregation reaction (3). It shows the dependence on the concentration C and the A parameter.

Equivalently, the calculated Gibbs free energy of deprotonation is:

$$\begin{aligned}\Delta_{\text{calc}}G &= -RT \ln K_{\text{calc}} = -RT \ln K_{\text{acid}} \\ &- RT \ln(AC + 1) = \Delta_{\text{acid}}G + \Delta_{\text{agg}}G\end{aligned}\quad (19)$$

Here the first component is the Gibbs free energy of deprotonation and the second component is the Gibbs free energy of aggregation:

$$\Delta_{\text{agg}}G = -RT \ln(AC + 1) = -RT \ln Agg \quad (20)$$

It is noteworthy that K_{calc} is dependent on the total concentration C of alkylamine added to the solution. The calculated and experimental alkylamine pK_a values are compared in Table 1 and in Figs. 3 and 4. Fig. 3 shows the dependence of observed pK_{obs} and calculated pK_{calc} on alkylamine chain length. Alkylamine pK_a values in the literature (obtained under non-aggregating conditions) are also plotted for comparison. Fig. 4 shows the dependence of observed pK_{obs} and calculated pK_{calc} on the total concentration of alkylamine. Experimental data match the calculated values quite well within the error of measurement.

The Gibbs free energy of aggregation depends on the standard reference state, such as molar or mole fraction standard states [17]. Without the reference state a value of the Gibbs free energy of aggregation is meaningless. This explains why we need to introduce two Gibbs free energies of aggregation ($\Delta_A G$, Eq. (8), and $\Delta_{\text{agg}} G$, Eq. (20)). First, the aggregation A Gibbs free energy ($\Delta_A G$) is unique for each alkylamine and can be conveniently listed in a literature with a defined reference state (1 M in this study). Second, the Gibbs free energy of aggregation ($\Delta_{\text{agg}} G$) is observed in the actual experiment where, for example, 2 mM concentration was used. It is necessary to define the concentration, because $\Delta_{\text{agg}} G$ is concentration-dependent. Both Gibbs free energies would be practically equal only if a hypothetical 1 M alkylamine concentration was used in the experiment.

3.7. Calculation of the concentrations of alkylamine forms during titration

To help visualize the appearance of the aggre-

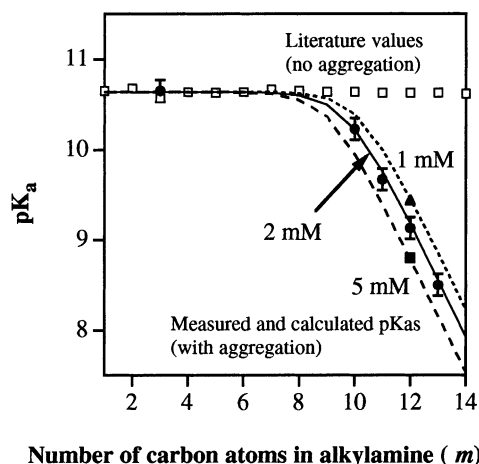


Fig. 3. Long chain alkylamine protonation pK_a dependence on alkyl chain length. Open squares show pK_a values of alkylamines in the literature [7]. They were obtained by extrapolating equivalent conductance measurements obtained in alcohol–water mixtures (prevents aggregation) to zero alcohol concentration [5]. Filled symbols — our experimentally determined pK_a values in aqueous solution at the following concentrations: \blacktriangle , 1 mM; \bullet , 2 mM; and \blacksquare , 5 mM. Lines show the calculated pK_a values according to the model (see text) at the following concentrations: dashed line with small intervals, 1 mM; solid line, 2 mM; and dashed line with large intervals, 5 mM.

gate at various pH values, we now calculate concentrations of all three alkylamine forms ($[\text{RNH}_3^+]$, $[\text{RNH}_2]$, and $[\text{RNH}_2 \downarrow]$) as a function of pH for various alkylamine chain lengths and various concentrations. We use Eqs. (4), (6) and (7) to express the concentrations of alkylamine forms in terms of the parameters of interest:

$$[\text{RNH}_3^+] = \frac{C 10^{-\text{pH}}}{10^{-\text{pH}} + (AC + 1)K_{\text{acid}}} \quad (21)$$

$$[\text{RNH}_2] = \frac{CK_{\text{acid}}}{10^{-\text{pH}} + (AC + 1)K_{\text{acid}}} \quad (22)$$

$$[\text{RNH}_2 \downarrow] = \frac{AC^2 K_{\text{acid}}}{10^{-\text{pH}} + (AC + 1)K_{\text{acid}}} \quad (23)$$

These concentrations are plotted as a function

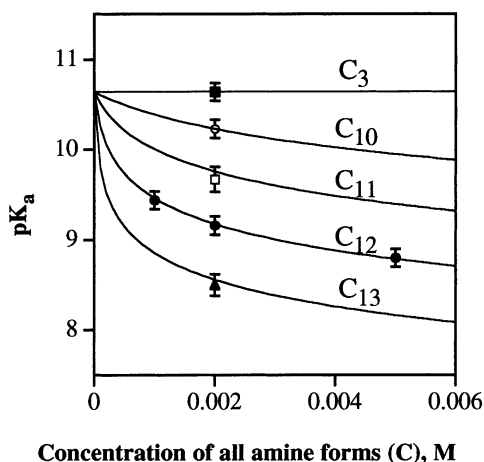


Fig. 4. Long chain alkylamine protonation pK_a dependence on concentration. Symbols represent our experimentally determined pK_a values in aqueous solution for the following alkylamines: ■, propylamine; ○, decylamine (C_{10}); □, undecylamine (C_{11}); ●, dodecylamine (C_{12}); and ▲, tridecylamine (C_{13}). Lines show the calculated pK_a values according to the model (see text).

of pH in Fig. 5. Such plots are generally known as Sillen diagrams [12]. Graphs on the left side show the dependencies for 2-mM concentrations of octylamine, decylamine, dodecylamine, and tetradecylamine. Concentration of the aggregate increases with increasing alkyl chain length, and the intersection between the upper two lines (approx. equal to the pK_{calc}) shifts to the lower pH. Graphs on the right side show the dependencies for 0.01, 0.1, 1 and 10 mM dodecylamine. As with increasing alkyl chain length, higher concentrations increase the relative fraction of the aggregate concentration and lower pK_{calc} .

Fig. 6 shows calculations for dodecylamine at concentrations below those we used in our experiments, indicating that some amount of aggregated RNH_2 is present even at the lowest concentrations. This small amount of aggregate may not be easily observable, but should be taken into account in the thermodynamic analysis of experiments.

3.8. Dependence of aggregation on temperature: van't Hoff analysis

To obtain the van't Hoff enthalpy and entropy

of aggregation, pH titrations were carried out at various temperatures. Fig. 7 compares propylammonium (C_3) and tridecylammonium (C_{13}) deprotonation curves obtained at 24.3 and 53.4°C. As in Figs. 1 and 2, the symbols are experimental data-points and the curves are simulated according to the model. The curves are shifted significantly with temperature, but their relative shapes are similar. Thus, aggregation was not affected in a major way: the temperature increase primarily affected K_{acid} and K_w . This introduces a potential for significant error in estimating the dependence of aggregation on temperature. However, careful analysis enabled determination of the temperature dependence of K_{acid} , K_w and A (Table 3).

Applying the van't Hoff equation to A or Agg we can obtain the enthalpy, entropy, and the heat capacity of aggregation. The derived enthalpy and the heat capacity are independent on the concentration C , but the entropy is dependent on the concentration.

$$\begin{aligned} \frac{\Delta_{agg} H_{vH}}{RT^2} &= \frac{\partial \ln Agg}{\partial T} = \frac{\partial \ln(AC + 1)}{\partial T} \\ &= \frac{C}{AC + 1} \frac{\partial A}{\partial T} \end{aligned} \quad (24)$$

or

$$\Delta_{agg} H_{vH} = \frac{\partial(\Delta_{agg} G/T)}{\partial(1/T)}$$

and when $AC \gg 1$, then

$$\frac{\Delta_{agg} H_{vH}}{RT^2} \approx \frac{\partial \ln A}{\partial T} \quad (25)$$

The constant pressure heat capacity is

$$\Delta_{agg} C_p = \frac{\partial \Delta_{agg} H_{vH}}{\partial T} \quad (26)$$

The entropy of aggregation is

$$\begin{aligned} \Delta_{agg} S &= - \frac{\partial \Delta_{agg} G}{\partial T} = R \ln(AC + 1) \\ &\quad + \frac{RTC}{AC + 1} \frac{\partial A}{\partial T} \end{aligned} \quad (27)$$

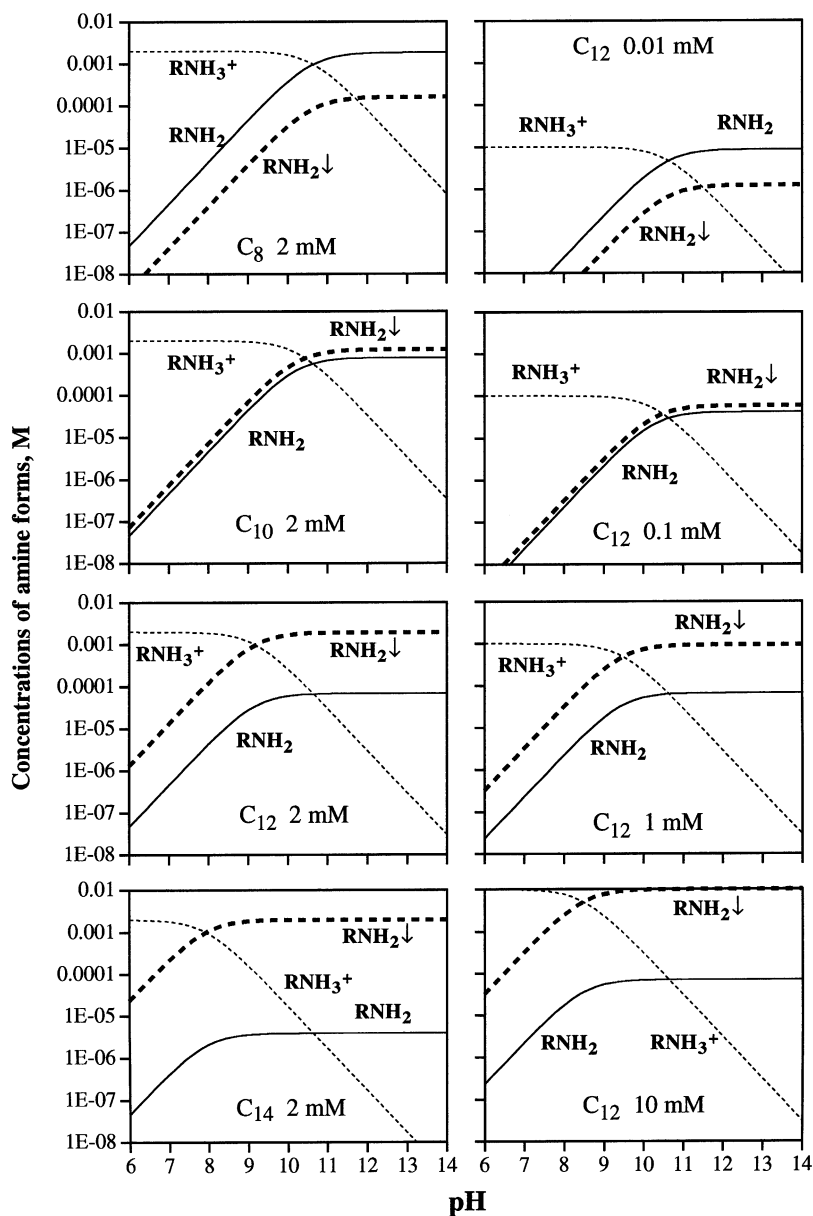


Fig. 5. Calculated concentrations of all three alkylamine forms as a function of pH (Sillen diagrams). Plots on the left side compare alkyl chain dependence from C_8 (upper left plot) to C_{14} (lower left plot), $C = 2$ mM. Plots on the right compare concentration dependence for dodecylamine (C_{12}) from 0.01 mM (upper right plot) to 10 mM (lower right plot). In the upper plots the amount of aggregate is negligible, and in the lower plots the amounts of the aggregate are sufficient to affect the pK_a values — intersections between upper two lines shift to the left. Small dashed lines — concentrations of the protonated alkylammonium cation (RNH_3^+), solid lines — concentrations of the neutral dissolved amine (RNH_2), and the broad dashed lines — concentrations of the aggregate ($RNH_2\downarrow$).

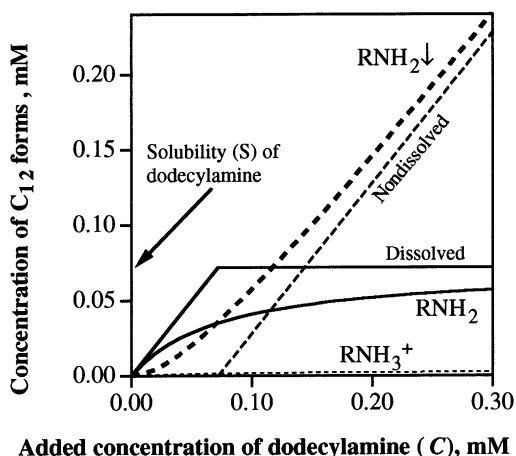


Fig. 6. Comparison between the phase approximation of solubility and our calculated concentrations of dodecylamine forms at pH 12, when $C \approx S$. All three forms of dodecylamine are present at all concentrations according to our model, while zero concentration of the aggregated phase is predicted by the phase approximation when $C < S$. However, when $C \gg S$, there is practically no difference between the two models.

$$\Delta_A S = - \frac{\partial \Delta_A G}{\partial T} = R \ln A + \frac{RT}{A} \frac{\partial A}{\partial T} \quad (28)$$

and when $AC \gg 1$, then

$$\Delta_{\text{agg}} S \approx \Delta_A S + R \ln C \quad (29)$$

The results for dodecylamine and tridecylamine aggregation at 24.3, 34.3, 43.1 and 53.4°C are shown in Table 3. Note that the aggregation parameters A obtained by curve fitting at 24.3°C differ slightly from the ones obtained by using Eq. (10). This discrepancy (17 000 or 14 100 for dodecylamine) shows the error of such estimates.

In Figs. 8 and 9 we have plotted the thermodynamic parameters for dodecylamine in comparison with the alkane dodecane as derived from its solubility dependence on temperature [18]. As noted above, ΔG and ΔS depend on concentration, so we have plotted them at $C = 2$ mM (Agg) and 1 M (A), the latter being the hypothetical standard state. On the other hand, ΔH and ΔC_p are independent of concentration. From this analysis we could conclude that the aggregation of dodecane is entropy-driven to a greater extent

than the aggregation of dodecylamine. However, as calorimetric analysis of dodecylamine aggregation reaction will show [10], van't Hoff analysis often gives unreliable enthalpies and entropies.

4. Discussion

We have demonstrated that the observed pK_a values of long chain n -aliphatic alkylamines are strongly perturbed by the linked aggregation reaction of deprotonated amine. This perturbation depends on both the concentration and the alkylamine chain length. When aggregation is taken into account, the pK_a values of all the studied alkylamines, regardless of chain length, are essentially the same. According to our model, the pH, at which the concentrations of dissolved amine forms equaled each other ($[RNH_3^+] = [RNH_2]$), was always equal to 10.64 (Fig. 5).

Aggregation thermodynamics is conventionally expressed through the solubility S or its reciprocal, the 'equilibrium constant' A , related to the molar free energy of transfer of alkylamine from solution to precipitate, $\Delta_A G = -RT \ln A$. However, the coupling of titration with aggregation in our experiments introduces an effective aggregation constant that depends on concentration, $Agg = AC + 1$. In our experiments with long-chain compounds, $AC \gg 1$, so the effective constant is proportional to concentration, an apparently paradoxical behavior whose explanation has required detailed analysis.

Solutions of sparingly soluble compounds are often approximated by a two-phase model. When the amount of added compound per volume of solution is below the solubility limit S , then the compound is assumed to dissolve fully. When the amount of added compound exceeds the solubility limit, then the excess compound is assumed to remain undissolved as another phase that is thermodynamically inactive. In our studies, when pH is sufficiently high to make the amount of the RNH_3^+ negligible, and when the concentration C is much higher than S , then the concentrations of RNH_2 and $RNH_2\downarrow$ follow closely the approximation described above. However, at low concentrations of alkylamine ($C < S$), the concentration

Table 3

Thermodynamic parameters of aggregation as a function of temperature for dodecylamine ($m = 12$) and tridecylamine ($m = 13$), and compared to data for dodecane (calculated from the solubility data in the literature)

Temp. (°C)	m^a	pK_w^b	pK_{acid}^c	A^d (M^{-1})	$\Delta_A G^e$ ($kJ\ mol^{-1}$)	$\Delta_{agg} G^f$	$\Delta_{agg} H_{vH}^g$	$\Delta_A S_{vH}^h$ ($J\ mol^{-1}\ K^{-1}$)	$\Delta_{agg} S_{vH}^i$	$\Delta_{agg} C_p^j$
24.3	12	14.02	10.84	17 000	−24.09	−8.79	−22.47	5.5	−46.3	−1006
	13	14.02	10.84	72 100	−27.66	−12.31	−12.00	52.5	0.9	−1072
	$C_{12}H_{26}$	–	–	4.60E7	−43.64	−28.27	−0.08	146.4	94.7	−875
34.3	12	13.72	10.73	11 500	−23.90	−8.12	−32.70	−28.3	−80.2	−1039
	13	13.72	10.73	55 200	−27.91	−12.05	−22.91	16.5	−35.1	−1108
	$C_{12}H_{26}$	–	–	4.35E7	−44.95	−29.07	−8.97	117.0	65.3	−904
43.1	12	13.50	10.35	8000	−23.63	−7.45	−41.99	−58.1	−110.0	−1069
	13	13.50	10.35	43 200	−28.07	−11.76	−32.80	−15.2	−66.9	−1140
	$C_{12}H_{26}$	–	–	3.76E7	−45.87	−29.53	−17.04	91.1	39.5	−930
53.4	12	13.30	9.85	4400	−22.78	−6.20	−53.20	−92.9	−145.0	−1104
	13	13.30	9.85	26 200	−27.62	−10.80	−44.73	−52.3	−104.0	−1177
	$C_{12}H_{26}$	–	–	2.90E7	−46.65	−29.78	−26.77	60.9	9.2	−960

^aNumber of carbon atoms in alkylamine (e.g. $m = 12$, dodecylamine).

^bNegative logarithm of the water ionization constant (K_w) at various temperatures used to simulate curves in Figs. 1, 2 and 7 according to Eq. (15), obtained from Butler and Cogley [12].

^cNegative logarithm of the alkylammonium deprotonation constant (K_{acid}) at various temperatures used to simulate curves in Figs. 1, 2 and 7 according to Eq. (15).

These constants are nearly identical to methylammonium deprotonation constants, obtained from Christensen et al. [23].

^dAggregation parameter A [Eq. (7)], obtained by regressing pH titration data against Eq. (15) where the only fitting parameter was A .

^eGibbs free energy of aggregation obtained from A using Eq. (8), $C = 1\ M$ (hypothetical).

^fExperimentally observed Gibbs free energy of aggregation, $C = 2\ mM$, calculated using Eq. (20).

^gVan't Hoff enthalpy of aggregation calculated using Eq. (24), independent of concentration.

^hVan't Hoff entropy of aggregation calculated using Eq. (28), $C = 1\ M$ (hypothetical).

ⁱVan't Hoff entropy of aggregation calculated using Eq. (27), $C = 2\ mM$.

^jVan't Hoff heat capacity of aggregation calculated using Eq. (26), independent of concentration.

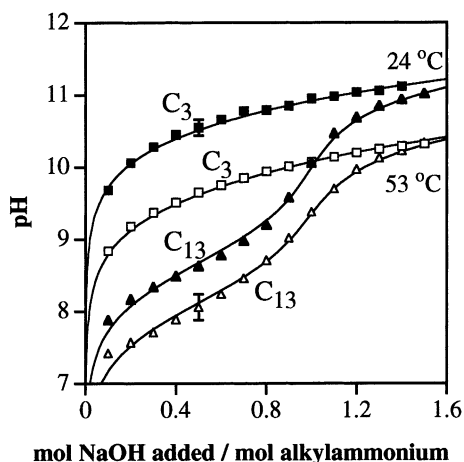


Fig. 7. Potentiometric titration curves of alkylammonium chlorides (2 mM) with sodium hydroxide (20 mM) at 24.3 (filled symbols) and 53.4 °C (open symbols). Datapoints are the experimentally observed results, squares — propylammonium, and triangles — tridecylammonium. Lines are calculated according to the model (see text) with a single fitting parameter A .

of aggregate is significant and not equal to zero (Fig. 6). When its concentration is very low, however, there is practically no impact on the pK_a of the alkylamine (0.01% for propylamine according to our calculations).

These results suggest that biophysical binding experiments should be carried out at several different concentrations. If the binding constant or other thermodynamic parameter is dependent on the concentrations of reactants at constant molar ratio, then one should look for a linked aggregation reaction, which may not be visible to the naked eye. Only if the binding parameters are concentration-independent can they be regarded as true thermodynamic parameters of a single molecular reaction.

A decrease in the pK_a value of an ionizable group upon changing its chemical environment can be explained in several ways. Dielectric permittivity (dielectric constant) of the environment may have changed affecting electrostatic

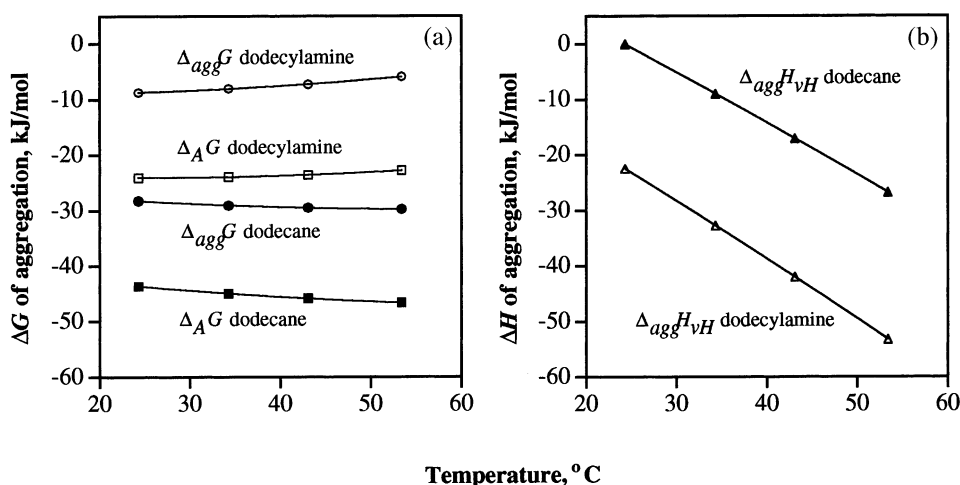


Fig. 8. Gibbs free energies (a) and enthalpies (b) of dodecylamine (open symbols) and dodecane (filled symbols) aggregation as a function of temperature. Symbols represent datapoints in Table 3 and the lines are second order polynomial fits. (a) Circles are experimentally observed ($C = 2$ mM) Gibbs free energies of aggregation ($\Delta_{agg}G$) and squares are $\Delta_A G$, $C = 1$ M. Gibbs free energies are practically independent of temperature. Data of great precision are needed to calculate temperature derivatives of the Gibbs free energy. (b) Triangles are van't Hoff enthalpies of aggregation as calculated from the Gibbs free energy dependence on temperature. Enthalpies are independent of concentration, therefore $\Delta_{agg}H = \Delta_A H$. Despite an apparent high precision, the enthalpy values are quite inaccurate as concluded from comparison with the calorimetric enthalpies of aggregation.

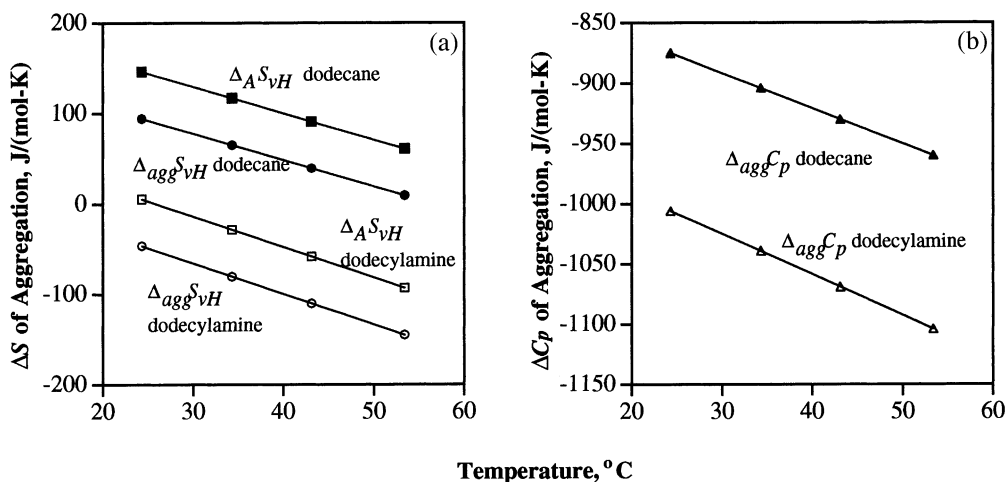


Fig. 9. Entropies (a) and heat capacities (b) of dodecylamine (open symbols) and dodecane (filled symbols) aggregation as a function of temperature. Circles are experimentally observed ($C = 2$ mM) entropies of aggregation ($\Delta_{agg} S$) and squares are entropies of aggregation at a hypothetical 1 M concentration ($\Delta_A S$). Entropies of aggregation decrease significantly and heat capacities of aggregation decrease slightly with increased temperature.

interactions between the charges. Additional charges may have been brought into the immediate vicinity of the first charge. Repulsion between charges of the same sign, or attraction between opposite charges, may affect protonation equilibria of both ionizable groups. However, in the case of alkylamines, we have shown that the pK_a shift was due to aggregation only. Upon deprotonation of long chain alkylamines, the amino headgroups were buried from aqueous solution by the surrounding neighboring molecules of the aggregate particle. Those buried molecules remained thermodynamically active and reversibly affected the apparent pK_a of the dissolved molecules by an amount proportional to the amount of material in the insoluble phase.

It is important to note that by titrating alkylammonium chlorides of intermediate chain lengths with hydroxide, the alkylamines were transferred from a nearly completely dissolved form to a nearly insoluble form. Critical micelle concentrations (CMC, molar) of alkylammonium chlorides at 25°C are expressed by the following empirical equation [19]:

$$\log \text{CMC} = 1.25 - 0.265m \quad (30)$$

where m is the number of carbon atoms in alkyl-

lammonium chloride. The CMC of dodecylammonium chloride, for example, is 11.7 mM, and that of tetradecylammonium is 3.47 mM. Thus, there are no micelles present at the beginning of titration at 2 mM alkylammonium concentration. At the end of titration, though, over 95% of dodecylamine and over 99% of tetradecylamine were in the aggregated form. There are very few such reactions in aqueous solution, where a hydrophobic alkyl compound is fully soluble at the beginning, and practically insoluble at the end of the reaction.

Alkylamine solubility and all thermodynamic parameters of aggregation could be calculated from pK_a shifts at various temperatures using van't Hoff analysis. However, as we shall show in the following paper [10] and as has been noted in other systems [20–22], the van't Hoff enthalpies and entropies often do not agree well with calorimetric data because of the inadequate precision even in careful measurements of the temperature dependence of the equilibrium constant. Still, van't Hoff analysis is widely used, and such analysis is the only way to obtain enthalpies and entropies when only Gibbs free energies can be measured.

This study presents three major conclusions.

Perhaps the most important is the finding that pK_a shift can be explained by aggregation and that the shift is a useful tool to study aggregation. We also have shown that the ‘concentration’ of non-dissolved compound, i.e. the amount of precipitate per volume of the solution, participates in thermodynamic equilibria and must be considered when interpreting the behavior of hydrophobic systems. Finally, the enthalpy and heat capacity of hydrophobic interactions are concentration-independent, but the Gibbs free energy and the entropy are dependent on concentration and may even change their sign.

Acknowledgements

This research was supported in part by NIH research grant GM28093.

References

- [1] B. Honig, A. Nicholls, *Classical electrostatics in biology and chemistry*, *Science* 268 (1995) 1144–1149.
- [2] N. Allewell, H. Oberoi, M. Hariharan, V. Li Cata, *Electrostatic Effects in Proteins: Experimental and Computational Approaches*, *Protein: A Comprehensive Treatise*, vol. 2, JAI Press, 1999, pp. 61–97.
- [3] W.R. Forsyth, M.K. Gilson, J. Antosiewicz, O.R. Jaren, A.D. Robertson, *Theoretical and experimental analysis of ionization equilibria in ovomucoid third domain*, *Biochemistry* 37 (1998) 8643–8652.
- [4] J.J. Dwyer, A.G. Gittis, D.A. Karp et al., *High apparent dielectric constants in the interior of a protein reflect water penetration*, *Biophys. J.* 79 (2000) 1610–1620.
- [5] C.W. Hoerr, M.R. McCorkle, A.W. Ralston, *Studies on high molecular weight aliphatic amines and their salts. X. Ionization constants of primary and symmetrical secondary amines in aqueous solution*, *J. Am. Chem. Soc.* 65 (1943) 328–329.
- [6] R.A. Robinson, R.H. Stokes, *Electrolyte Solutions*, Butterworths Scientific Publications, London, 1955, p. 499.
- [7] D. Lide (Ed.), *CRC Handbook of Chemistry and Physics*, CRC Press, Boca Raton, 2000.
- [8] J.A. Dean, *Lange’s Handbook of Chemistry*, 15th ed, McGraw-Hill, Inc, New York, 1999.
- [9] C. Tanford, *The Hydrophobic Effect: Formation of Micelles and Biological Membranes*, John Wiley and Sons, New York, 1980.
- [10] D. Matulis, V.A. Bloomfield, *Thermodynamics of the hydrophobic effect. II. Calorimetric measurement of enthalpy, entropy, and heat capacity of aggregation of alkylamines and long aliphatic chains*, *Biophys. Chem.* 93 (2001) 53–65.
- [11] D. Matulis, *Thermodynamics of the hydrophobic effect. III. Condensation and aggregation of alkanes, alcohols, and alkylamines*, *Biophys. Chem.* 93 (2001) 67–82.
- [12] J.N. Butler, D.R. Cogley, *Ionic Equilibrium. Solubility and pH Calculations*, John Wiley and Sons Inc, New York, 1998.
- [13] R.G. Bates, *Electrometric pH Determinations. Theory and Practice*, John Wiley & Sons, New York, 1954.
- [14] F.M. Jones, E.M. Arnett, in: A. Streitwieser, Jr., R.W. Taft (Eds.), *Thermodynamics of Ionization and Solution of Aliphatic Amines in Water*, vol. 11, John Wiley & Sons, New York, 1974, pp. 263–322.
- [15] C. McAuliffe, *Solubility in water of paraffin, cycloparaffin, olefin, acetylene, cycloolefin, and aromatic hydrocarbons*, *J. Phys. Chem.* 70 (1966) 1267–1275.
- [16] C. McAuliffe, *Solubility in water of normal C9 and C10 alkane hydrocarbons*, *Science* 163 (1969) 478–479.
- [17] M.H. Abraham, *Thermodynamics of solution of homologous series of solutes in water*, *J. Chem. Soc. Faraday Trans. 1*, 80 (1984) 153–181.
- [18] C.L. Yaws, *Chemical Properties*, McGraw-Hill, New York, 1999.
- [19] I.J. Lin, *CMC of flotation reagents and its relation to HLB*, *Trans. Soc. Mining Eng., AIME* 250 (1971) 225.
- [20] Y. Liu, J.M. Sturtevant, *Significant discrepancies between van’t Hoff and calorimetric enthalpies, II*, *Protein Sci.* 4 (1995) 2559–2561.
- [21] H. Naghibi, A. Tamura, J.M. Sturtevant, *Significant discrepancies between van’t Hoff and calorimetric enthalpies*, *Proc. Natl. Acad. Sci. U.S.A.* 92 (1995) 5597–5599.
- [22] Y. Liu, J.M. Sturtevant, *Significant discrepancies between van’t Hoff and calorimetric enthalpies, III*, *Biophys. Chem.* 64 (1997) 121–126.
- [23] J.J. Christensen, L.D. Hansen, R.M. Izatt, *Handbook of Proton Ionization Heats*, John Wiley and Sons, 1976.